

Analysis on the Influence of Gap Flow Around a Tractor-Trailer

Yue Yang, Jinxing Chen, Yuqi Huang*, Jiangang Chen, Yuan Ji
 Power Machinery & Vehicular Engineering Institute,
 Zhejiang University,
 Hangzhou 310027,
 China
 E-mail: huangyuqi@zju.edu.cn

ABSTRACT

With the booming of electronic commerce and logistics industry, tractor-trailers play an increasingly important role in transport industry. However, as tractor-trailers are large consumers of energy, this issue arouses the attention of scholars and manufacturers to reduce their energy consumption due to the global energy crisis. For tractor-trailers, aerodynamic drag accounts for a large proportion of total resistance, thus reduction of aerodynamic drag is an efficient energy-saving method. Among various kinds of aerodynamic drag, the gap flow between truck and trailer has a relatively large impact, which has attracted people's attention. Due to the great differences in structures and sizes of trucks, it is of great significance to find out the optimal gap between truck head and carriage to get the best aerodynamic characteristics.

This paper aims to explore the optimum gap of each model and analyze the mechanisms and laws of the flow. The Ahmed reference model was established, without considering other factors, such as wheels, wing mirrors and so on. The grid division was done with ICEM software. By comparing the CFD numerical simulation results in ANSYS FLUENT with the wind tunnel experiment, the established model was evidenced to be correct and reliable. Three typical tractor-trailers were chosen and simplified as models with different area ratios of truck and trailer. The turbulent flow around models was investigated with LES (Large Eddy Simulation) model to discuss the influence on aerodynamic characteristics caused by gap between truck and trailer. It is indicated by the research that there was a best gap for minimal coefficient of drag (C_D) about per model. In conclusion, when the height of trucks does not exceed that of trailers, it has the minimal C_D when the area ratio is close to one. The relationship among gap, C_D and area ratio provides a meaningful reference for the design of trucks in efficiently reducing fuel consumption and greenhouse gas emission.

NOMENCLATURE

C_D	[-]	Coefficient of drag
C_L	[-]	Coefficient of lift
C_P	[-]	Coefficient of pressure
u	[m/s]	Velocity
f	[N·m ³ /kg]	Body force
p	[Pa]	Pressure
t	[s]	Time
A	m ²	Windward area
D	N	Drag force
L	N	Lift force
x	[m]	Cartesian X axis direction
y	[m]	Cartesian Y axis direction
z	[m]	Cartesian Z axis direction

Special characters

μ	[Pa·s]	Dynamic viscosity
ν	[m ² /s]	Kinematic viscosity
ρ	[kg/m ³]	Density
ψ	[-]	Area ratio
g	[m]	Gap distance

Subscripts

max	Maximum
wn	Wall-normal direction
i	ith direction
j	jth direction

INTRODUCTION

As the main component of the total resistance in automobile, aerodynamic drag attracts much attention for many years. It has been found by NAGAYUKE MARUSHI (1991) [1] in Automobile Technology Handbook that aerodynamic drag accounts for half of the whole drag when the car is moving at the speed above 60km/h. Accordingly, improving the aerodynamic characteristic of vehicles could efficiently reduce energy consumption, especially for tractor-trailers which are big consumers of energy. Previous studies [2] suggested if C_D decreased by 30%, 12%-13% of fuel consumption would be saved. Considering the high ratio of trucks and huge consumption of diesel per year, small improvement on aerodynamic performance could bring about great economic benefits.

Currently, wind tunnel experiment and computational fluid dynamics (CFD) are two main methods of studying aerodynamics. CFD has advantages of low expense, short time circle, good reproducibility and visualization feature which make the analysis of flow field around vehicles much easier.

Previous studies [3] by CFD methods show that the aerodynamic drag of track-trailer mainly consists of frictional resistance and pressure drag, the latter one accounts for more than 50%. When airflow hits the upper edge of the carriage, it forms a separation bubble and finally creates a high-pressure region. Meanwhile, the flow separates at the rear of the truck, emerging vortex structure, which leads to huge energy dissipation and creates a low-pressure region. The pressure difference between front and rear of truck causes great resistance.

Due to the requirement of truck's transportation usage, streamline shape could not be applied in heavy trucks to reduce air drag like small cars. At present, one main way to improve the aerodynamic characteristic of trucks is attaching aerodynamic packages to reduce the area of high pressure region and eliminate the vortex at the rear of trucks. Harun Chowdhury (2013) [4] noticed that the external attachments

(fairing and covering) had notable impact on aerodynamic drag which could reduce around 26% aerodynamic drag over the baseline model. Alamaan Altaf (2014) [5] studied different shapes of rear flaps and found elliptical flaps had the best effect. However, all these aerodynamic packages do not solve the problem from the original structure of tracker-trailer. What's more, there would be an extra cost to attach packages.

It is obvious that the gap between truck head and carriage impede the smoothness of airflow, but there is few researches about the gap flow between truck and trailer. Zheng Zhiying (2010) [6] found that the 1:10 model had the smallest C_D when the gap was 55mm. However, Zheng's research only focused on one model and no other factors were taken into consideration. In actual usage, there are various kinds of trucks which have various area ratios of truck and trailer and the optimized gap might be totally different.

To study the mechanism of gap flow and explore the rules of the resistance variation Vs. gap at different area ratio, several three-dimensional models were established and discussed in this paper. The Large Eddy Simulation (LES) model was adopted to analyze the flow around truck and trailer after the method was validated by the comparison of simulation and experimental results on Ahmed model.

METHODOLOGY

Several turbulence models have been developed to solve the simulation problem on turbulence flow, such as Direct Numerical Simulation (DNS), Reynolds Average Navier-Stokes (RANS), Large Eddy Simulation (LES) and so on. LES based on the assumption that flow of small scale is homogenous and isotropic. LES divides the turbulent flow into large eddies and small eddies, the large eddies are simulated directly, while the influence of small eddies are solved by Subgrid-Scale (SGS) model. The simulation by LES could get more detailed information of flow field than by RANS, and cost less computing resources than by DNS. Therefore, LES is appropriate for present study.

There are several kinds of SGS model of LES: Smagorinsky-Lilly model, Wall-Adapting Local Eddy-Viscosity Model (WALE), Algebraic Wall-Modeled LES Model (WMLES) and Dynamic Kinetic Energy Subgrid-Scale Model (KET), where the WMLES was selected in this paper. WMLES uses RANS within the boundary layer while the outer area is simulated by LES. This method could not only lower the requirement of mesh density, but also guarantee the accuracy of computing results.

The turbulent flow of incompressible Newtonian fluid is described by Navier-Stokes equations as follows [7]

$$\frac{\partial u_i}{\partial t} + \frac{\partial u_i u_j}{\partial x_j} = -\frac{1}{\rho} \frac{\partial p}{\partial x_i} + \nu \frac{\partial^2 u_i}{\partial x_i \partial x_j} + f_i, \quad (1)$$

$$\frac{\partial u_i}{\partial x_i} = 0. \quad (2)$$

In LES, the large-scale quantities are defined by filter operations [7] which are used to separate large eddied from small ones.

$$\bar{f}(x) = \int f(x') G(x, x') dx' \quad (3)$$

where, $G(x)$ are filter function, of which most commonly used is cutoff filter expressed as [7]

$$\hat{G}_i(k_i) = \begin{cases} 1 & k_i \leq K_i \\ 0 & \text{otherwise} \end{cases} \quad (4)$$

in which, $\hat{G}_i(k_i)$ is the Fourier coefficient of the filter function in the direction of i , $K_i = \pi/\Delta_i$ is the cutoff wave number, and Δ_i is the filter width in the in the direction of i .

Applying filter operation to Navier-Stokes equations will get the governing equations of LES model which are expressed as [7]

$$\frac{\partial \bar{u}_i}{\partial t} + \frac{\partial \bar{u}_i \bar{u}_j}{\partial x_j} = -\frac{1}{\rho} \frac{\partial \bar{p}}{\partial x_i} + \nu \frac{\partial^2 \bar{u}_i}{\partial x_i \partial x_j} - \frac{\partial \tau_{ij}}{\partial x_j}, \quad (5)$$

$$\frac{\partial \bar{u}_i}{\partial x_i} = 0 \quad (6)$$

in which, τ_{ij} is the SGS stress which represents the exchange of momentum between large eddies and small ones, expressed as flows [7]

$$\tau_{ij} = \bar{u}_i \bar{u}_j - \bar{u}_i \bar{u}_j \quad (7)$$

To solve the governing equations, τ_{ij} must be modeled to close the equation which are computed from [7]

$$\tau_{ij} - \frac{1}{3} \tau_{kk} \delta_{ij} = -2\nu_t \bar{S}_{ij} \quad (8)$$

in which, τ_{kk} is the isotropic part of SGS stress which is not need to be modeled. \bar{S}_{ij} is the rate of strain tensor which is defined as [7]

$$\bar{S}_{ij} = \frac{1}{2} \left(\frac{\partial \bar{u}_i}{\partial x_j} + \frac{\partial \bar{u}_j}{\partial x_i} \right) \quad (9)$$

ν_t is the SGS turbulent viscosity, in WMLES model, it is calculated by [8]

$$\nu_t = (C_{SMAG} \Delta)^2 \{1 - \exp[-(y^+/25)^3]\} S, \quad (10)$$

$$\Delta = \min\{\max[C_W d_w, C_W h_{max}, h_{wn}], h_{max}\}. \quad (11)$$

In the above equations, S is the magnitude of the strain tensor, y^+ is the normal to the wall inner scaling, C_{SMAG} is equal to 0.2. Δ is the sub grid length scale defined by (10), where C_W is an empirical constant which equals to 0.2, d_w is the distance to the wall, h_{wn} is the grid step in the wall-normal direction and h_{max} is the maximum grid step.

METHOD VALIDATION

To validate the reliability of this method, Ahmed model which has been acknowledged in aerodynamics field was selected as contrast object. Ahmed model is a generic ground vehicle model which could reflect the basic features of flow around vehicles with the ignorance of engine compartment, wing mirrors and other surface bulges. It was designed by SR Ahmed (1984) [9] to analyze the time-averaged automotive wake vortex and finally discovered that the flow around the body is influenced by the slant angle of rear surface. D.B. Sims-Williams (2001) [10] found the uniqueness of Ahmed model and further applied it to unsteady flow. S. Krajnovic (2005) [11] simulated the flow field around Ahmed model by Large Eddy Simulation and provided reference for future studies.

The geometric shape of Ahmed model is shown in Figure 1, in which θ is the angle of slant surface, the length of the model is 1044mm, the height is 288mm, the width is 389mm, the length of the slant surface is 222mm and the model is located 50mm above the ground. The flow structure is mainly defined by the angle of slant surface. Considering that the 25° model is close to the critic angle 30° and has a more complex flow condition, thus the flow field of 25° model was discussed carefully.

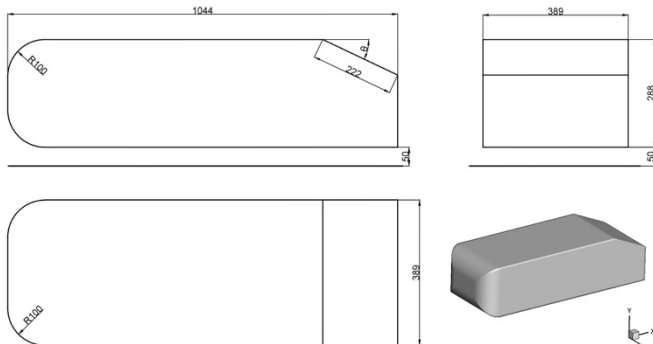


Figure 1 Geometric diagram of Ahmed reference model

The computational domain and mesh as shown in Figure 2 and Figure 3 were generated in ICEM program. The length of model is defined as L , where the length of computational domain is $7L$, the width is $10W$, and the height is $8L$. (L , W , H represent the length, width, height of Ahmed model respectively). The velocity inlet is $1.5L$ distant upstream from the front surface of the model and the outlet is $4.5L$ distant downstream from the model.

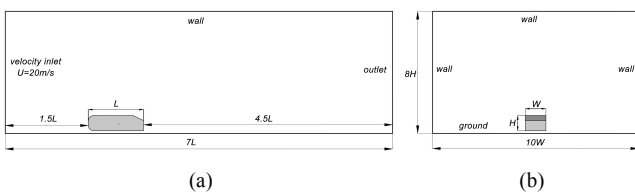


Figure 2 Dimensions of computational domain

(a) Side view (b) rear view

The simulation adopted structured grid as shown in Figure 3(a). The total number of grids is approximately 5.85 million. To satisfy the strict requirements of LES model's mesh, the grids of near wall region were densified through using O-grid, as shown in Figure 3(b). Y plus value is around 1 to meet the requirements of near wall grid.

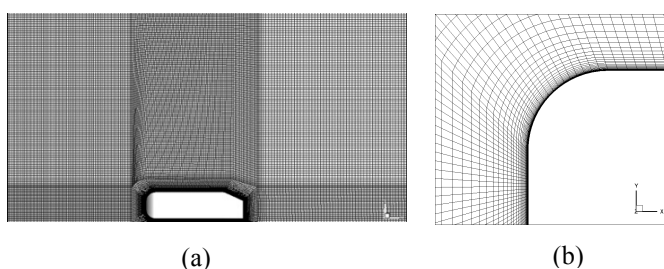


Figure 3 Computational mesh

The boundary conditions of computational domain were determined in solver ANSYS FLUENT 16.5. The velocity of inlet was 20m/s, the outlet condition was pressure out of where the gage pressure was 0. The ground was defined as moving wall of which the velocity was 20m/s relative to the model. The

walls and the surface of Ahmed model were defined as no slip wall. The Reynold number of the flow is 1.17×10^6 calculated by

$$Re = \frac{Ul_D}{\nu} \quad (12)$$

where, U is the velocity at inlet which is 20m/s, l_D is the length of Ahmed model which is 1044mm, ν is the kinematic viscosity of air in 15 °C which is 1.789×10^{-5} m²/s

WMLES S- Ω model was selected as the simulation method. The scheme of pressure-velocity coupling was defined as SIMPLEC. The spatial discretization method of gradient was least squares cell based and that of pressure was set as second order, of momentum is second order upwind. Transient calculation was adopted to simulate the flow, of which the time step size is 0.001s and the total number of time step is 2,000. The formulation of transient was defined as second order implicit.

Table 1 demonstrates the comparison of C_D and C_L of simulation with experimental results. The C_D of 25° model simulated by LES is 0.295 where the error is around 3.5% compared to the wind tunnel experiment by Ahmed (1984) [9] and the error of C_L is around 5.5%. The results show that WMLES is precise enough and suitable for this research.

Table 1 Comparison of C_D and C_L

	Simulation result	Experimental result	Error (%)
C_D	0.295	0.285[9]	3.5%
C_L	0.378	0.400[9]	5.5%

The flow structure and characteristics of 25° model are shown as following figures and compared with the results of Liu Xun [12]. It can be learnt from Figure 4 which shows the velocity vector that the results in this paper is nearly the same as that in comparative literature. Two vortexes are formed at the rear of the model, the upper vortex flows in clockwise direction, while the under vortex flows in anti-clockwise direction and the two vortexes construct the separation bubble described by SR. Ahmed (1984) [9]

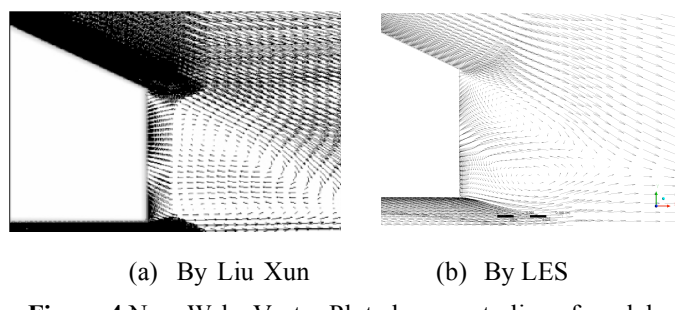


Figure 4 Near Wake Vector Plot along centerline of model

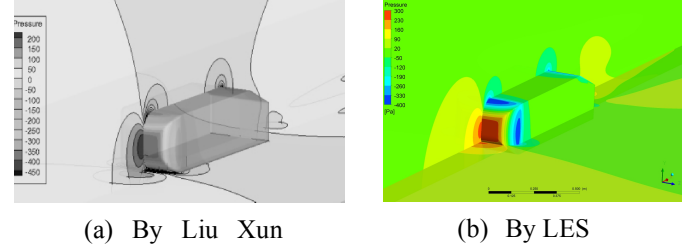


Figure 5 Front Side View of Pressure Field

Figure 5 demonstrates the pressure field of the simulation. The results of comparative literature and that of LES both show the same characteristics that there is a high-pressure region in the front of model, with low-pressure regions at the margins of model's head and the slant surface where the flow separates.

In conclusion, with all the comparisons and analysis above, the LES method of this paper is reliable and valid.

MODEL ESTABLISHMENT

Three real trucks were chosen as prototypes and 1:1 simplified models were drawn to analyze the gap follow around tract-trailers. The three chosen trucks are of the same capacity which is 40 tons and the size of carriage is identically equal that is 9.6 meters long, 4 meters in height and 2.5 meters wide. The primary difference among them is the height of truck head which bring about diverse area ratio of truck and trailer, as well as different aerodynamics characteristics.

FAW JIEFANG J6P heavy truck (CA4250P66T1A2E22M-4), of which the total length is 12 meters and 2.5 meters in width. The height of truck head is 3.2 meters and the area ration of truck and trailer is 0.8:1, shown in Figure 6 (a). JAC GALLOP K5 truck (HFC4181P1K5A35S7V) is 3.56 meters high, of which the area ratio is 0.89:1, shown as Figure 6 (b). DONGFENG TIANLONG (DFL5253XXYAX1B), of which the truck head is 4 meters high, the area ratio is 1:1 shown as Figure 6 (c).

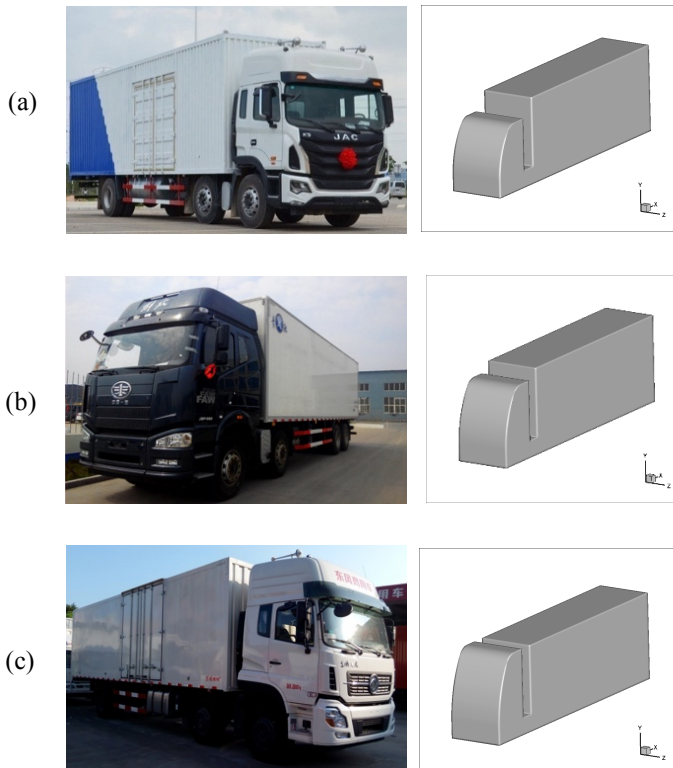


Figure 6 Picture of Referenced Real Truck and Simplified Model
(a) FAW JIEFANG J6P (b) JAC GALLOP K5 (c) DONGFENG TIANLONG

The basic geometric parameters of the model are shown in Figure 7. The gap distance between truck head and carriage is defined as g , of which the unit is meter. Considering the width of truck head and that of carriage are even, thus the area ratio can be calculated by the height of truck head (H_h) and carriage

(H_c). The dimensionless parameter ψ represent the area ratio. The paper studied these three models with seven different gap distances (0.3m, 0.55m, 0.60m, 0.65m, 0.70m, 0.75m, 1m) and thus 21 cases were generated. The boundary conditions were the same as the settings of Ahmed model in method validation with 20 m/s inlet velocity. The number of grids are around 5.2 billion.

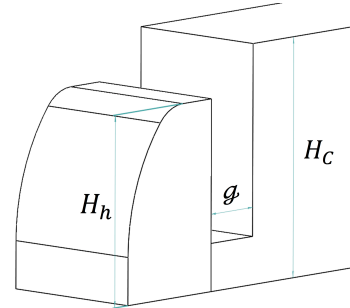


Figure 7 Geometric diagram of model

RESULTS AND DISCUSSION

Figure 8 reflects the relationship among area ratio, C_D and gap distance. The results of various gaps all reveal that coefficient of drag decreases with the rising of area ratio and the discrepancy is obvious which means area ratio has a dramatic impact on aerodynamic drag. Considering the influence of gap distance, Figure 10 reflects that the three curves all reflect a tendency of firstly declining and then rising which means there is an optimal gap of each model for minimal C_D . In cases of $\psi=0.8$ and $\psi=0.89$, the distance with minimum C_D is 0.65m and that of $\psi=0.89$ is 0.6 m. The value of C_D increase rapidly when distance is above 0.65m.

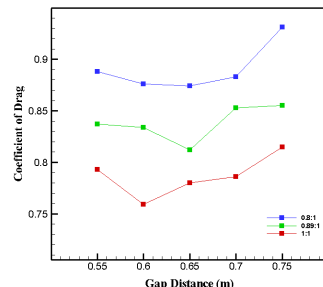


Figure 8 C_D in different gaps

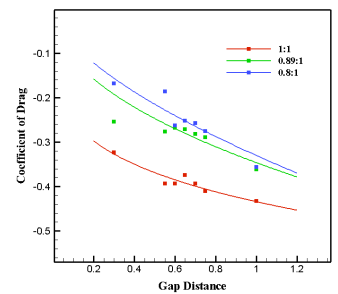


Figure 9 C_L in different gaps

The link between C_L and area ratio is demonstrated in Figure 9 that C_L also has a negative correlation with area ratio. The models with larger area ratio have smaller C_L which represents higher downforce. There is little difference of C_L between $\psi=0.8$ and $\psi=0.89$, while the value C_L is obviously smaller in cases of $\psi=1$. As can be learnt from Figure 8 and 9 that models with higher area ratio have better aerodynamic characteristics for smaller air drag and bigger downforce. When comparing the cases of different gaps, it shows a negative relationship between gaps and C_L that models with smaller gap distance have minor down force.

Figure 10 shows the surface pressure contours of models with three different area ratios in same gap distance. The three models all reflects a high-pressure region at the truck head which is the primary cause of drag forth and the size of region is due to the different height of truck head. A low-pressure region exists at the upper part of truck head of all models in which the airflow separates. The size of negative region

increases with the rising of area ratio which means higher truck head has better ability of guiding flow. The models with area ratio of 0.8 and 0.89 both have a positive pressure region at the top edge of trailer, while this region does not exist in contour of model with 1:1 area ratio. The high-pressure located in the top edge of carriage could be a critical factor to increase the airflow resistance and deteriorate aerodynamics characteristics.

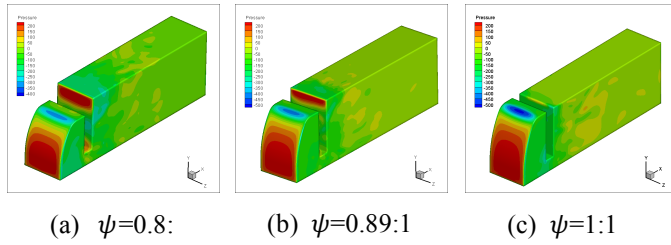


Figure 10 Surface Pressure Contour

Figure 11 is the velocity contour of XY slice along the center of 15 cases. Comparing the cases horizontally about the influence of area ratio, it can be concluded that, with the rising of ψ , more high-speed air flows into the gap, while contour (c) shows almost no existence of high velocity air. Low-speed airflow is generated above the carriage in contours (a) (b) which means vortex is formed in this region. The flow passes the gap of models with 1:1 area ratio more smoothly and does not engender low-speed air above the carriage. The vertical comparison of the cases shows that the high-speed air flows into the gap increases with the rising of g , which is an important factor to cause the deterioration of drag resistance. In contours (c), of which area ratio equals to 1, it shows no obvious change of high-speed in the gap area which could be explained by the better guiding ability of higher truck head. In cases of small gap, more low-speed airflow is above carriage which means flow separation is more severe of models with smaller g .

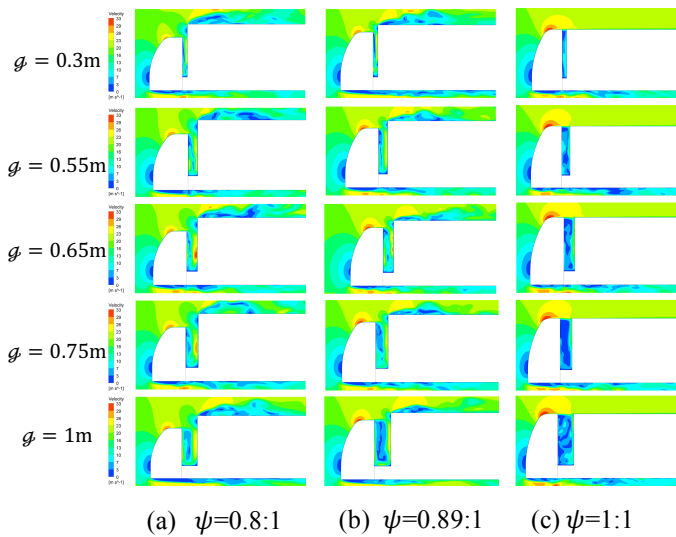


Figure 11 Velocity Contour of XY slice

The vorticity condition demonstrated in Figure 12 reveals that the gap and region above carriage are high-vorticity areas. The comparison of contours with different area ratio reflects that with the increasing of ψ , the vortex in the gap and the vortex intensity of models with 0.89:1 area ratio shown in Contour (b) is weaker than (a), while Contour (c) is the weakest. The existence of vortex exacerbates the dissipation of energy and brings about larger drag resistance. The cases with three different ψ all embody the same trend that with the increasing of g , the vorticity in the gap intensifies greatly which could lead

to the increasing of C_D . Although the contours of smaller gap show the existence of higher peak value of vorticity which could be explained by the impediment of narrow gap, the total intensification of vortex is larger in models with bigger g for greater air intake. The vorticity above the carriage shows a opposite tendency of gap. Without the transitional region provided by relatively large gap, the airflow of cases with smaller gaps separates greatly when it flows past the carriage. Synthesizing Figure 14 and 15, it could be concluded that larger gap distance will increase the air flows into the gap and enhance the vortex intensity, finally being reflected as the rising of C_D . Smaller gap could enhance the flow separation above the carriage which will decrease the down force.

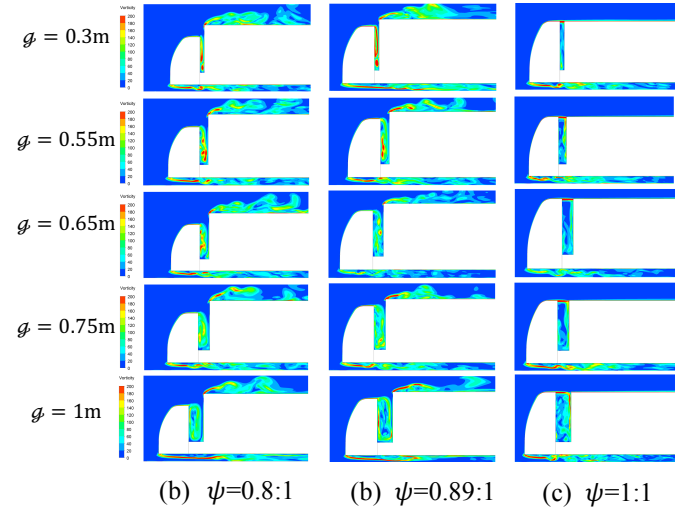


Figure 12 Vorticity Contour of XY slice

Figure 13 demonstrates the coefficient of pressure along the centerline of top and bottom surface. The three curves in Figure 13 have almost the same changing trend but the red curve of 1:1 area ratio is smoother than the other two which could explain that airflow of 1:1 model flows past the gap more fluently. The blue and green curve fluctuate violently within the X/L range from 0.2 to 0.4 where is the front top area of carriage, which means the flow is very instable in this area. Models with 1:1 area ratio has relatively larger C_P of top surface ($X/L=0.2\sim 1$). Figure 13 (b) is the C_P of bottom surface along the centerline, the three curve have the same tendency of rising while the red curve ($\psi=1$) has relatively larger C_P . The larger C_P on the top of carriage and smaller C_P at bottom could explain models with 1:1 ratio have bigger downforce and smaller C_L .

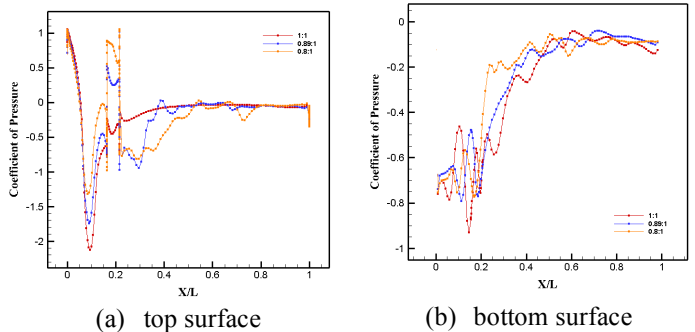


Figure 13 C_P along the centerline

The three curves tend to overlap in the end shown in Figure 13 reveals that the pressure at the rear of models is almost the same, thus the discrepancy of C_D could be resulted from the pressure difference of truck head. Figure 14 is the enlarged

figure of C_p of along the centerline of truck head and the gap. It can be concluded from this figure that the curves of higher area ratio simultaneously have larger value of C_p . The C_p of model with 0.8:1 area ratio (green curve) is the largest, the second followed by 0.89:1 model and 1:1 model has the smallest C_p . The higher C_p in the truck head ($X/L=0\sim0.1$) and the gap ($X/L=0.15\sim0.23$) leads to larger drag resistance.

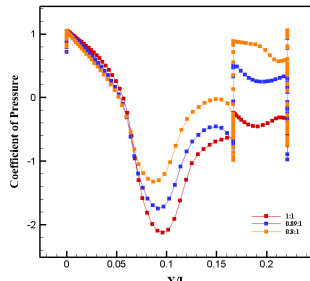


Figure 14 C_p along the centerline of truck head and gap with different area ratio

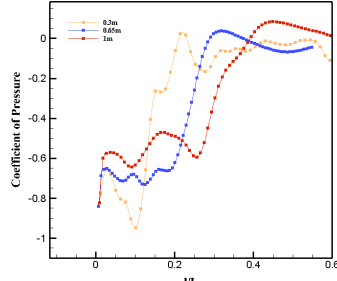
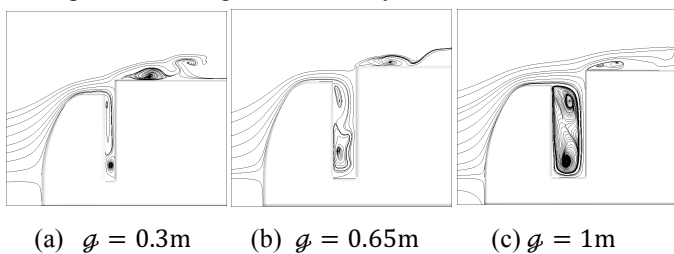


Figure 15 C_p along the centerline of carriage with different gaps

Figure 15 shows the C_p of carriage centerline of different gaps with same area ratio. The red curve ($g = 1m$) is above the blue and green curves within $X=0\sim0.2$ which means there is less intense flow separation above the carriage. The green curve fluctuates greatly within $X=0\sim0.2$ and has a minimum value of C_p which means airflow separates severely because of the relatively shorter transitional region before the impedance of carriage. The C_p of upper surface of carriage is higher in large gap than in small ones which explains models with larger gaps have greater down force.

The streamline along the centerline shown in Figure 16 reflects the same trend that the vortex in the gap is strengthened with the increasing of gap distance. Models with relatively big gaps provide sufficient space for the generation of large eddy, while narrow gap limits the intake of airflow and thus relatively small eddy is formed. The flow separation above the carriage is greater in cases of smaller gaps and the separation exhibits downward trend with the increasing gap which means the air flows past the carriage more fluently.



(a) $g = 0.3m$ (b) $g = 0.65m$ (c) $g = 1m$

Figure 16 Streamline along the centerline

CONCLUSION

The paper analyzed the influence of gap flow by using computational fluid dynamics method and found some mechanism and laws of flow characteristics. The area ratio between truck head and carriage has a significant impact on the aerodynamics characteristics. Trucks with smaller area ratio have larger coefficient of drag because of the high-pressure region caused by the air impingement on the carriage. Relatively smaller down force also exists in models with larger area ratio for strong flow separation above the carriage. To improve the aerodynamics of trucks, great height difference

between truck head and carriage should be avoided.

The increasing of gap distance between head and carriage could enlarge the vorticity in the gap and lead to larger drag force. While small gaps could cause severe flow separation above the carriage and result in the rising of C_L . In conclusion, both too big and too small gaps could deteriorate the aerodynamics. The paper found that models with gap around 0.6~0.65m have the best aerodynamics for relatively smaller C_D and C_L which could provide reference for future design of trucks. The difference of C_D between the largest and smallest model is up to 19%. It has also been found that the optimal gap is different of models with different area ratio due to different air intake of the gap and the various smoothness of flow past the carriage. Due to the limitation of numbers of studied objects, the specific relationship between the optimal gap and area ratio could be studied in the future.

REFERENCES

- [1] NAGAYUKE MARUSHI, etc. Automobile technology handbook. The first edition, June, 15, 1992.
- [2] Fu Limin. Automotive Aerodynamics. China Machine Press, 2006.
- [3] ZHENG Zhiying, BAI Zhe, XU Hongpeng, BO Zemin, CAI Weihua, LI Fengchen. Study on Drag Reduction Characteristics of Hole-drilled Aerodynamic Device Attached in the Rear of Van. *Energy Conservation Technology*. Vol.29, Sum. No. 166. Mar.2011, No.2.
- [4] Harun Chowdhury, Hazim Moria, Abdulkadir Ali, Iftekhar Khan, Firoz Alam and Simon Watkins. A study on aerodynamic drag of a semi-trailer truck. *Procedia Engineering* 56, 2013, pp. 201-205.
- [5] Alamaan Altaf, Ashraf A. Omar, Waqar Asrar. Passive drag reduction of square back road vehicles. *J. Wind Eng. Ind. Aerodyn.* 134, 2014, pp. 30-43.
- [6] ZHENG Zhiying, BAI Zhe, XU Hongpeng, BO Zemin, CAI Weihua, LI Fengchen. Study on the Effect of the Distance Between the Front and the Compartment of Van Its Aerodynamic Characteristics. *Energy Conservation Technology*. Vol.28, Sum. No.164. Nov.2010, No16.
- [7] Ugo Piomelli, William H. Cabot, Parviz Moin, and Sangsan Lee. Subgrid-scale backscatter in turbulent and transitional flows. *Phys. Fluids A*, Vol. 3, NO. 7, July 1991. pp. 1766-1771.
- [8] Mikhail L. Shur^a, Philippe R. Spalart^b, Mikhail Kh. Strelets^a, Andrey K. Travin^a. A hybrid RANS-LES approach with delayed-DES and wall-modelled LES capabilities. *International Journal of Heat and Fluid Flow*. No.29, 2008, pp. 1638–1649.
- [9] Ahmed, S., Ramm, G., and Faltin, G. Some Salient Features of The Time-Averaged Ground Vehicle Wake. *SAE Technical Paper*. 840300, 1984.
- [10] Sims-Williams D.B. Self-Excited Aerodynamic Unsteadiness Associated with Passenger Car, A Thesis submitted for the degree of Doctor of Philosophy, University of Durham, 2001.
- [11] S. Krajnovic and Lars Davidson. Flow around a simplified car, Part1: Large eddy simulation, *Journal of Fluid Engineering*, Vol. 127, 2005, pp. 907-918.
- [12] LIU Xun, LAI Chen-guang. Numerical Simulation Research of External Flow Field on Ahmed Model. *Journal of Chongqing University of Technology (Natural Science)*. Vol. 27, No. 9, Sep. 2013.

